HHS Public Access

Author manuscript

Sci Signal. Author manuscript; available in PMC 2022 April 18.

Published in final edited form as:

Sci Signal. ; 14(696): . doi:10.1126/scisignal.abc9012.

Dimeric form of CXCL12 binds to atypical chemokine receptor 1

Julia C. Gutjahr[1,†], **Kyler S. Crawford**[2,†], **Davin R. Jensen**[2], **Prachi Naik**[1], **Francis C. Peterson**[2], **Guerric P. B. Samson**[3], **Daniel F. Legler**[3,4], **Johan Duchene**[5], **Christopher T. Veldkamp**[6], **Antal Rot**[1,5,7,*], **Brian F. Volkman**[2,*]

[1]Centre for Microvascular Research, William Harvey Research Institute, Barts and The London School of Medicine and Dentistry, Queen Mary University of London, London EC1M 6BQ, UK

[2]Department of Biochemistry, Medical College of Wisconsin, Milwaukee, WI 53226, USA.

[3]Biotechnology Institute Thurgau (BITg) at the University of Konstanz, 8280 Kreuzlingen, Switzerland.

[4]Theodor Kocher Institute, University of Bern, Bern, Switzerland.

[5]Institute for Cardiovascular Prevention, Ludwig-Maximilians University, 80336 Munich, Germany.

[6]Department of Chemistry, University of Wisconsin-Whitewater, Whitewater, WI 53190, USA.

[7]Centre for Inflammation and Therapeutic Innovation, Barts and The London School of Medicine and Dentistry, Queen Mary University of London, London EC1M 6BQ, UK.

Abstract

The pleiotropic chemokine CXCL12 is involved in diverse pathophysiological processes, including embryogenesis, hematopoiesis, leukocyte migration and tumor metastasis, while apparently engaging only one classical and one atypical receptor, CXCR4 and ACKR3, respectively. Here we show that CXCL12, though primarily in its dimeric form, is also able to bind to the atypical chemokine receptor 1 (ACKR1), previously known as Duffy antigen/receptor for chemokines, or DARC. Using nuclear magnetic resonance spectroscopy and isothermal titration calorimetry, we demonstrate that dimeric CXCL12 binds to the extracellular N-terminus of ACKR1 with low nanomolar affinity, while the binding affinity of the monomeric CXCL12 is orders of magnitude lower. The CXCL12 dimer, but not the monomer, efficiently binds to cellular ACKR1, as shown using ACKR1-transfected cells and primary human Duffy-positive erythrocytes. In summary, we report a new interaction between CXCL12 dimer and ACKR1, which provides another layer of regulation of multiple biological functions of CXCL12. The ability of ACKR1 to bind CXCL12 and potentially also other chemokines in their dimeric form

*To whom correspondence should be addressed: bvolkman@mcw.edu, or a.rot@qmul.ac.uk.
†these authors contributed equally

Author contributions:
Conception and design: JCG, CTV, AR, BFV
Development of methodology: JCG, CTV, KSC, FCP, GPBS, DFL
Acquisition of data: JCG, KSC, DRJ, PN, FCP, GPBS, CTV
Analysis and interpretation of data: JCG, KSC, DRJ, PN, FCP, GPBS, DFL, JD, CTV, AR, BFV
Writing of the manuscript: JCG, KSC, CTV, AR, BFV
Review and/or revision of the manuscript: JCG, KSC, DRJ, PN, FCP, GPBS, DFL, JD, CTV, AR, BFV
Administrative, technical, or material support: DFL, AR, BFV Corresponding authors: AR, BFV

Competing interests: BFV and FCP have ownership interests in Protein Foundry.

offers new insights into mechanisms behind known functions of ACKR1 in chemokine retention and presentation in the bone marrow and on venular endothelial cells.

One Sentence Summary:

Atypical chemokine receptor 1 binds to dimeric CXCL12, suggesting additional roles in chemokine retention and presentation.

Keywords

CXCL12 homodimer; ACKR1; erythrocytes

Introduction

Chemokines are a group of intercellular communication proteins that bind to their classical cognate G-protein coupled receptors (GPCRs) to initiate different cell responses, most commonly directed migration (1). In addition, chemokines engage atypical chemokine receptors, which regulate chemokine availability in defined microenvironments by sequestering and scavenging or transporting and presenting cognate chemokines (2). Homeostatic chemokines such as CXCL12 are constitutively expressed to maintain discrete cellular niches. CXCL12 is also known as stromal cell-derived factor 1 (SDF-1) as it was first described as a Pre-B-cell growth-stimulating factor expressed by bone marrow stromal cells (3-5). Mice deficient for CXCL12 die prenatally, showing severe developmental defects in hematopoiesis as well as defects in cardiac ventricular septa formation (6). These phenotypes of CXCL12 knockout mice are shared by mice deficient for both CXCL12 receptors, G-protein coupled CXCR4 (7, 8) and atypical chemokine receptor 3 (ACKR3) (9, 10). Due to multifaceted and broad functional involvement of CXCL12, it is key to understand the mechanisms which regulate its distribution and function, including post-translational modifications and other molecular interactions (11). Secreted CXCL12 readily forms homodimers, which have altered receptor-binding preference as compared to the monomeric form and activate differential signal transduction pathways downstream of CXCR4 (12-14). Therefore, the monomer-dimer equilibrium of CXCL12 significantly influences the functions of this chemokine. Here we describe a novel interaction of CXCL12 with the atypical chemokine receptor 1 (ACKR1) which clearly differs for the monomeric and dimeric forms of this chemokine.

ACKR1 was first discovered on red blood cells (RBCs) as the Duffy blood group antigen (15). It was subsequently shown to be exploited as an entry receptor for *Plasmodium vivax* and *Plasmodium knowlesi* invasion of RBCs (16-19), whereby ACKR1 induces the dimerization of its malarial parasite ligand the Duffy-binding protein (DBP) (20-22). The recognition that Duffy antigen also binds inflammatory chemokines of CC and CXC families (23-25) led to its designation as Duffy antigen/receptor for chemokines or DARC (26), an acronym widely used until its recent classification as an atypical chemokine receptor (2) and subsequent inclusion in the systemic nomenclature (27). A prevalent ACKR1 polymorphism present in the majority of individuals of African ancestry abolishes its expression on RBC (28), thus conferring a resistance to *P. vivax* and *P. knowlesi* malaria

(17). In addition to RBCs and their bone marrow precursors (29), ACKR1 is also expressed by the endothelial cells (30, 31) of post-capillary venules (32, 33) and by non-vascular cells including the Purkinje neurons of the cerebellum (31, 34). Individuals who lack ACKR1 on RBCs still express it in the endothelial cells and in the brain (26). ACKR1 on RBC acts as chemokine sink and reservoir, buffering the spikes in free plasma chemokines but also extending their half-life (35-38), thus shaping leukocyte responses to a broad range of chemokines, including by direct cross-competition for binding by chemokines with differential affinities for ACKR1 (39). Based on our current findings, the paradigms of ACKR1-mediated control of chemokine availability and function can now be extended to include the regulation of CXCL12.

The interaction between ACKR1 and CXCL12 was first suggested by protein nuclear magnetic resonance (NMR) spectroscopy, showing binding of the ACKR1 N-terminus to CXCL12, which was highly preferential for the dimeric form of chemokine. ACKR1 binding of CXCL12 dimer, but not monomer, was confirmed by isothermal titration calorimetry (ITC) and measurement of fluorescent chemokine binding using cellular systems of ACKR1 expression. ACKR1 preferential affinity for CXCL12 dimers might represent a new, unexpected pathway to regulate the relative availability of the monomeric and dimeric chemokine forms of CXCL12 in distinct, characteristic microenvironments of CXCL12 and ACKR1 expression (40, 41).

Results

Protein NMR spectroscopy

Chemokines are thought to interact with their receptors through a two-site, two-step binding and activation model, though more advanced models describe additional steps and subsidiary binding events (42-44). However, all models agree that a chemokine interacts with its receptor's extracellular N-terminus either followed by or preceded by other interactions with different portions of its G-protein coupled receptor (GPCR). Given the role of the chemokine receptor N-terminus in chemokine binding, protein NMR has successfully investigated the interaction of chemokines and the N-termini of many of the signaling chemokine GPCRs (45-50). Therefore the interaction of the N-terminus of ACKR1 with wild type CXCL12 (CXCL12-WT) and its locked monomeric and dimeric variants, denoted here as CXCL12-LM (51, 52) and CXCL12-LD (45), respectively, was investigated using protein NMR. A sixty-amino acid peptide corresponding to the extracellular N-terminus of ACKR1, denoted ACKR1$^{N\text{-}term}$, was expressed recombinantly and purified. Standard three-dimensional protein NMR techniques (21, 53) confirmed backbone atom assignments for [U-^{15}N/^{13}C] ACKR1$^{N\text{-}term}$ (Fig. 1A). ^{15}N-^{1}H HSQC spectra were used to monitor the titration of [U-^{15}N] ACKR1$^{N\text{-}term}$ with incremental additions of unlabeled CXCL12-LM, CXCL12-WT, or CXCL12-LD. Overlays of the spectra from the titrations are shown in Fig. 1B-D. Consistent with binding of WT CXCL12 or its variants, upon titration many ACKR1$^{N\text{-}term}$ residues show chemical shift changes and/or broaden beyond detection. Fig. 1E-G are plots of ACKR1$^{N\text{-}term}$ chemical shift perturbations induced by 200 μM CXCL12-LM, CXCL12-WT or CXCL12-LD. All three chemokines induce chemical shifts changes or peaks that broaden beyond detection for ACKR1$^{N\text{-}term}$ residues in the twenties as indicated

with the red bars in Fig. 1E-G. CXCL12-WT and, to a greater extent, CXCL12-LD lead to broadening of additional ACKR1$^{N\text{-}term}$ peaks with many of these located in the fifties region of ACKR1$^{N\text{-}term}$ residues. Previous reports provide contradicting claims regarding the interaction or lack thereof of CXCL12 with ACKR1 (54, 55). Our analysis of the ACKR1$^{N\text{-}term}$ spectra suggests that ACKR1$^{N\text{-}term}$ can bind CXCL12-LM, CXCL12-WT and CXCL12-LD with potentially significant differences in affinity and stoichiometry.

To confirm ACKR1$^{N\text{-}term}$ binding to CXCL12, [U-^{15}N] CXCL12-LM, [U-^{15}N] CXCL12-WT, and [U-^{15}N] CXCL12-LD were titrated with unlabeled ACKR1$^{N\text{-}term}$ and monitored by 2D NMR. Overlays of ^{15}N-^{1}H HSQC spectra of CXCL12-LM, CXCL12-WT, and CXCL12-LD with increasing concentrations of ACKR1$^{N\text{-}term}$ are shown in Fig. 2A-C. Binding of ACKR1$^{N\text{-}term}$ to CXCL12-LM induced chemical shift perturbations on a fast exchange time scale with a subset of peaks showing incremental changes in chemical shift upon additions of ACKR1$^{N\text{-}term}$ (Fig. 2A). CXCL12-WT exhibited a similar, but non-identical, pattern of ACKR1$^{N\text{-}term}$-induced shifts with pronounced peak broadening at intermediate titration points (Fig. 2B). In contrast to CXCL12-LM and CXCL12-WT, additions of ACKR1$^{N\text{-}term}$ to CXCL12-LD produced extreme peak broadening leading to the disappearance of many signals (Fig. 2C).

Perturbations induced by 400 μM ACKR1$^{N\text{-}term}$ for observable residues in CXCL12-LM, CXCL12-WT and CXCL12-LD are quantified in Fig. 2D-F, with amino acids that broaden beyond detection indicated in red and with a value of 2.5 in the graph. Chemical shift perturbations were mapped onto the structure of CXCL12 in Fig. 2G with an interaction schematic in Fig. 2H (45). The predicted binding site of the N-terminal peptide includes residues adjacent to the dimerization interface of wild type CXCL12, and in the dimer overlaps the structured chemokine core, involving the adjacent α-helices of each monomer but not residues in the chemokine N-termini. While the chemical shifts indicate binding to all three CXCL12 variants, the interaction between ACKR1$^{N\text{-}term}$ and CXCL12-LD is different and, potentially, of a greater affinity than its interaction with CXCL12-LM or CXCL12-WT.

Binding events resulting in continuous NMR peak shifts (fast exchange on the chemical shift time scale) as observed for ACKR1$^{N\text{-}term}$ binding to CXCL12-LM typically correspond to rapid dissociation kinetics and lower affinity (56). Slower off rates associated with intermediate exchange (CXCL12-WT) or extreme peak broadening (CXCL12-LD) are often correlated with higher binding affinities. Chemical exchange broadening in the CXCL12-WT titration could also arise from a shift in the monomer-dimer equilibrium if, for example, ACKR1$^{N\text{-}term}$ bound preferentially to CXCL12 dimer. While NMR titration data is often used to estimate K_D values in the μM to mM range, the disappearance of signals from the CXCL12-LD spectrum precluded quantitative comparisons of ACKR1$^{N\text{-}term}$ binding affinity to the different oligomeric states of CXCL12.

High affinity ACKR1$^{N\text{-}term}$ binding to the CXCL12 dimer

Isothermal titration calorimetry (ITC), a sensitive technique for direct measurement of the thermodynamics of biophysical binding events, was used to further characterize the interaction between ACKR1$^{N\text{-}term}$ and CXCL12 or its variants. ITC confirmed the notion

that the ACKR1$^{N\text{-}term}$ bound CXCL12-LD with higher affinity than CXCL12-WT and CXCL12-LM (Fig. 3A-C). For CXCL12-WT and CXCL12-LD, saturation of ACKR1$^{N\text{-}term}$ binding occurs near a 1:1 molar ratio, with CXCL12-LD showing a complex isotherm for which the full dataset could not be fitted to a simple binding model. ITC measurements fitted using Origin with a one-site binding model for CXCL12-WT yielded a mean K_D of 4.0 ± 1.0 μM (Fig. 3D). ITC determination using CXCL12-LD showed an initial high affinity interaction that was approximated using a sequential binding model. The first transition yielded a mean K_D of 0.006 ± 0.01 μM. Titration of CXCL12-LM with ACKR1$^{N\text{-}term}$ did not evolve heats capable of being fitted or characteristic of a high-affinity interaction. Recall CXCL12-WT exists in a monomer-dimer equilibrium (57). The locked monomer and locked dimer results would suggest CXCL12-WT dimer can bind the ACKR1$^{N\text{-}term}$ tightly while monomer would not. Interestingly, fitting of the CXCL12-WT ACKR1$^{N\text{-}term}$ interaction showed an *n*, or number of sites, of approximately 0.5 (Fig. 3D) indicating a binding stoichiometry of two chemokines to one ACKR1$^{N\text{-}term}$. Although the possibility of ACKR1$^{N\text{-}term}$ binding two monomers cannot be excluded, this strongly suggests ACKR1$^{N\text{-}term}$ binding would promote dimerization of CXCL12-WT. These results are consistent with previous observations of the propensity of CXCL12 to dimerize upon binding to heparin or the CXCR4 receptor N-terminus (46, 57). This is further supported by an *n* number of sites of approximately 1 for the interaction of CXCL12-LD with ACKR1$^{N\text{-}term}$ (Fig. 3D). Here, an *n* of 1 indicates a one to one interaction between CXCL12-LD, which is structurally analogous to CXCL12-WT dimer, and ACKR1$^{N\text{-}term}$ (45). Taken together, the NMR and ITC results show ACKR1$^{N\text{-}term}$ binds CXCL12-WT and CXCL12-LD and suggests ACKR1$^{N\text{-}term}$ promotes and preferentially binds CXCL12 dimer.

CXCL12 binding to full-length cell surface ACKR1

Next, we tested CXCL12 binding to ACKR1 expressed in a cellular system first using MDCK cells stably transfected with human ACKR1. Flow cytometry using a specific monoclonal anti-human ACKR1 antibody showed that after transfection, the MDCK cells highly expressed ACKR1 (Fig. 4A). Fluorescently-labeled CCL2, a canonical high-affinity ligand of ACKR1 (58, 59), was used to confirm chemokine-binding activity of ACKR1 in transfected MDCK cells. Live cell confocal microscopy imaging as well as flow cytometry clearly showed that only the ACKR1-transfected MDCK, but not the control cells, were able to bind and, with time, internalize CCL2-AF647 (Fig. 4B and C).

As biochemical measurements indicated that ACKR1 preferentially binds CXCL12-LD, we directly labeled this chemokine with a fluorophore AF647 and used live cell confocal imaging to compare its binding to ACKR1-transfected and control MDCK cells. CXCL12-LD-AF647 bound only to the ACKR1-transfected MDCKs in which it initially co-localized with ACKR1 on the cell surface (Fig. 5A). Labeling ACKR1-MDCK cells with CXCL12-LD-AF647 followed by a prolonged incubation at 37 °C, led to chemokine internalization. The ACKR1 immunoreactivity remained prominently associated with the cell membranes, which at later timepoints were devoid of CXCL12-LD-AF647 found scattered intracellularly, partially co-localizing with ACKR1 (Fig. 5A). Next, we used flow cytometry to compare the binding of CXCL12-LD-AF647 and CXCL12-WT-AF647 to ACKR1-deficient and -sufficient MDCK cells. CXCL12-LD-AF647 associated

with ACKR1-expressing MDCK cells significantly more than CXCL12-WT-AF647, and both chemokines bound significantly better to ACKR1-expressing MDCK cells than control MDCKs (Fig. 5B). CXCL12-LD-AF647 had also higher than CXCL12-WT-AF647 ACKR1-independent, non-specific binding. Furthermore, the highest concentrations of both dimeric and WT cross-competed, though not very efficiently, for ACKR1 binding of fluorescently-labeled canonical chemokine ligand CCL2-AF647, with CXCL12-LD competing to a significantly greater extent than CXCL12-WT (Fig. 5C).

Duffy-positive erythrocytes preferentially bind CXCL12-LD

To test the interaction of CXCL12-LD-AF647 with ACKR1 expressed in the membranes of primary human cells, we investigated the binding of the dimeric CXCL12 to erythrocytes of Duffy-positive individuals which, as anticipated, showed prominent ACKR1 expression on their surface (Fig. 6A and fig. S1A). The erythrocytes of Duffy-negative individuals were used as negative controls, as these cells are practically devoid of ACKR1 expression (Fig. 6A and fig. S1A). Accordingly, Duffy-positive but not Duffy-negative erythrocytes could bind CCL2-AF647 (fig. S1B). Confocal microscopy was used to observe the pattern of CXCL12-LD-AF647 binding to erythrocytes of Duffy-positive and Duffy-negative individuals. Upon addition of CXCL12-LD-AF647 to erythrocyte suspension, fluorescence was first associated with the fluid phase in both Duffy-positive and Duffy-negative samples. However, already after 10 min incubation at 37 °C, fluorescent chemokine bound to Duffy-positive erythrocytes and remained associated with their surface, without signs of internalization, for three hours duration of the experiment. Conversely, CXCL12-LD-AF647 failed to significantly associate with Duffy-negative erythrocytes, thus illustrating the ACKR1-dependence of erythrocyte binding dimeric CXCL12. Fig. 6A presents a direct morphological comparison of CXCL12-LD-AF647 interaction to Duffy-positive and Duffy-negative erythrocytes initially and following a one-hour incubation.

Next, we used Duffy-positive and Duffy-negative erythrocytes to quantify and compare the ACKR1-binding capacity of fluorescently-labeled CXCL12-LD-AF647 and CXCL12-WT-AF647. These experiments clearly demonstrated the ACKR1-mediated binding of CXCL12-LD-AF647, which dose-dependently associated with erythrocytes of Duffy-positive individuals while Duffy-negative erythrocytes showed negligible binding (Fig. 6B). However, due to considerable variations between individual donors, the differences were statistically significant only for the highest chemokine concentration used (Fig. 6B). CXCL12-WT-AF647 also bound to Duffy-positive erythrocytes, but significantly less than CXCL12-LD. Surprisingly, Duffy-negative erythrocytes bound significantly more CXCL12-WT-AF647 than CXCL12-LD-AF647 with WT CXCL12 binding equally well to Duffy-positive and -negative cells (Fig. 6B). Such hierarchical pattern of ACKR1-independent erythrocyte binding of CXCL12 variants could be consistent with the involvement of CXCR4 and/or ACKR3, both receptors showing preference for the monomeric CXCL12 over the dimeric one (14). However, this is clearly not the case, as erythrocytes do not express these receptors, neither the classical CXCR4 (fig. S2), nor the atypical ACKR3 (60). The observed ACKR1-independent binding of the WT chemokine theoretically could also be mediated by sulfated sugars, heparan sulfate in particular, known to interact with chemokines and impinge on their localization (61, 62). Heparan sulfate is expressed on

erythrocyte membranes (63), but its involvement in selective binding of CXCL12-WT-AF647 is not likely, as it preferentially binds dimeric vs. monomeric CXCL12 (64). It is possible that, in addition to CXCR4, ACKR3, ACKR1 and heparan sulfate, CXCL12 binds to yet another unidentified molecule present on the erythrocyte surface.

In subsequent binding competition experiments, the ACKR1-dependent erythrocyte binding of CCL2-AF647 was dose-dependently inhibited by increasing concentrations of CXCL12-LD, but not CXCL12-WT, reaching statistical significance at the highest concentration used, although, at the highest concentration tested, inhibiting only approximately 20% of CCL2-AF647 binding (Fig. 6C).

In conclusion, ACKR1 expressed in cellular context in transfected cells and by primary erythrocytes bound efficiently only the dimeric form of CXCL12, which also competed with CCL2 for ACKR1 binding, though not very potently or efficaciously, but significantly better than its WT counterpart. These data provide a potential explanation why previous studies on ligand specificity of ACKR1, which relied on competition binding by a series of wild-type chemokines (54), overlooked CXCL12 as a potential ligand, a potent binder as a dimer, but a relatively weak competitor, even in its dimeric form.

Discussion

CXCL12 forms an extensive protein-protein interface with the flexible N-terminal domain of its receptors CXCR4 and ACKR3 (44, 51, 65). ACKR1 has the longest N-terminal domain in the chemokine receptor family (60 amino acids) and binds a multitude of inflammatory chemokines, but apparently not homeostatic chemokines like CXCL12 (54), a notion that was recently contested by Klei *et al.* (55). While most chemokines form dimers at micromolar concentrations or in the presence of glycosaminoglycans (66-68), they are generally understood to bind their G protein-coupled receptors as monomers (69, 70). However, we discovered previously that the CXCR4 N-terminus binds both monomeric and dimeric CXCL12 with near-equal affinity (45). Since previous surveys of chemokine-ACKR1 binding typically relied on measurements of competitive displacement of a high-affinity probe (e.g. CXCL8, CXCL1, or CCL2) (29, 54, 71, 72), we investigated the direct binding of CXCL12 to the ACKR1 N-terminal domain and found that ACKR1 exhibited a strong preference for binding to the dimeric form of CXCL12. Post-translational modification of ACKR1 includes glycosylation and sulfation, facilitating oligomerization of malarial DBP (21, 73). In CXCR4, glycosylation of Asn^{11} and sulfation of Tyr^{21} increase CXCL12 binding and dimerization (45, 74-76). The recombinant ACKR1 fragment produced in bacteria lacks those modifications, which are more likely to enhance CXCL12 binding than to diminish or alter it. Our findings confirm a recent report that CXCL12 is an ACKR1 ligand (55), but also significantly modify its conclusions as monomeric CXCL12 is not a potent ligand of ACKR1. Our data opens a possibility that other chemokines which apparently fail to compete with canonical ACKR1 ligands for binding might still bind ACKR1 in physiologically relevant contexts. Furthermore, it is also possible that canonical inflammatory chemokine ligands of ACKR1 also preferentially bind in their dimeric form.

Only the ACKR1 interaction with the malarial DBP has been structurally characterized, where residues Gln^{19}-Tyr^{30} bind as an α-helix at the DBP dimer interface (27). Chemical shift perturbations suggest this region of ACKR1, which contains a cluster of acidic residues and a tyrosine (Tyr^{30}) conserved among orthologs that is sulfated to bind DBP oligomers, also binds CXCL12 and its locked oligomeric variants. However, ACKR1 residues between His^{52} and Asp^{59} are also implicated in the binding to CXCL12-WT or CXCL12-LD. We speculate that ACKR1 employs multiple epitopes within its flexible N-terminus to bind dimeric CXCL12 with nanomolar affinity, perhaps explaining why this interaction was overlooked in previous studies. Comparison with crystal structures of CXCR4, CCR5, and CXCR2 (69, 77, 78) illustrates a conserved interaction between the receptor N-terminus and chemokine residues forming a groove between the N-loop and 40s loop. If ACKR1 binds chemokines using different subsets of its N-terminal domain, ligand displacement assays would likely yield variable or discordant results depending on the combination of labeled chemokine probe and competing ligand.

Mapping ACKR1 induced chemical shift perturbations onto the surface on CXCL12-LD was hampered by the disappearance of signals in the HSQC spectrum, which may be a consequence of the high affinity of this interaction or the formation of higher-order complexes. Residues of CXCL12-WT with the largest ACKR1-induced perturbations include key CXCR4-recognition residues (e.g. Val^{49} and Cys^{50}) (46), so we hypothesize that the CXCL12 receptor binding surfaces are at least partially overlapping. However, the large number of shifted CXCL12-WT HSQC peaks also includes residues Val^{23}, Val^{49}, and Thr^{31} bracketing the dimer interface (e.g. β1 strand, α-helix), suggesting that ACKR1 promotes dimerization of the chemokine, consistent with the 2:1 binding stoichiometry obtained by ITC. ACKR1 binding has been reported to induce dimerization of the malarial DBP by forming contacts with both subunits at the dimer interface in the crystal structure, thus providing a potential target for antibody therapy and anti-malarial vaccines (20, 22, 79). Although ACKR1 itself has also been reported to homodimerize- and heterodimerize with CCR5 (80), our stoichiometry data shows that CXCL12 dimers are interacting with monomeric rather than dimeric ACKR1.

CXCL12 is a long-established soluble regulator of hematopoiesis that is presumed to act via its widely expressed receptor CXCR4 (6). More recently, we demonstrated that ACKR1 on the surface of nucleated erythroid cells also regulates hematopoiesis but relevant ligands remained undefined (29). Dimerization of CXCL12 is a highly relevant modification that contributes complexity to chemokine homeostasis in microenvironments with high CXCL12 concentration, such as bone marrow. While the diversity of chemokines is usually the mode of eliciting complex cellular responses through GPCRs, a precise balance of CXCL12 levels in the bone marrow modulates stem cell retention as well as healthy and malignant hematopoiesis (81). However, concentrations of CXCL12 high enough to favor dimerization may also interfere with monomeric signaling, as dimeric CXCL12 has altered CXCR4 affinity and signals through alternate pathways compared to the monomeric form (14). Our results suggest that one of the potential unexpected new functions of ACKR1 involves binding CXCL12 dimers, thus immobilizing and/or removing them from discrete cellular microenvironments. The sites of ACKR1 expression in the bone marrow include erythroid cells, positioned in direct contact with hematopoietic stem and

progenitor cells, and vascular endothelial cells of the sinusoids (29), the sites of constitutive intense cell trafficking into and from the bone marrow. Thus, ACKR1, modifying the monomer-dimer equilibrium of CXCL12, might regulate the effects these CXCL12 variants in physiological and pathological hematopoiesis and bone marrow cell outputs. Future investigation into ACKR1 binding affinity for CXCL12 as influenced by other possible post-translational modifications, like truncation by CD26/DPP-IV digestion or chemokine hetero-oligomerization as well as the ability of ACKR1 to bind dimeric forms of other chemokines, may uncover its additional regulatory functions in chemokine homeostasis. These findings are likely relevant for ACKR1 function in other tissues, including cerebellar neurons (82) and endothelial cells of post-capillary venules, where ACKR1 provides for optimal chemokine-induced leukocyte emigration into the tissues (33, 83).

Materials and Methods

Chemokine production

Wild type CXCL12 (CXCL12-WT) exists in a concentration-dependent monomer-dimer equilibrium (57). CXCL12 locked monomer (CXCL12-LM) remains monomeric in isolation even at high concentrations due to L55C and I58C mutations but is structurally similar to wild type CXCL12 monomer as previously described (52). CXCL12 locked dimer (CXCL12-LD) remains dimeric at low concentrations due to L36C and A65C mutations, yet remains structurally similar to wild type CXCL12 dimer as previously described (45). CXCL12-LM, CXCL12-LD, and CXCL12-WT were expressed and purified using the protocol published in (Veldkamp *et al.* 2016) (84). The identity of CXCL12, CXCL12-LM, CXCL12-LD and CCL2 was confirmed by linear ion trap quadrupole mass spectrometry (LTQ-MS). Lyophilized proteins were stored at −20° C.

CXCL12-WT, CXCL12-LD and CCL2 were fluorescently labeled using a two-step process employing sortagging (85) and copper-catalyzed azide-alkyne click chemistry. Expression plasmids for CXCL12-WT, CXCL12-LD and CCL2 were modified using the polymerase chain reaction to contain a C-terminal sortase A recognition motif with the amino acid sequence LPETGG. DNA sequence of the CXCL12-WT-SORT, CXCL12-LD-SORT and CCL2-SORT expression plasmids were confirmed by DNA sequencing. Expression and purification of the SORT containing variants was as described for the wild-type proteins (45). The identity of CXCL12-WT-SORT, CXCL12-LD-SORT and CCL2-SORT was confirmed by LTQ-MS. Purified proteins were lyophilized and stored at −20° C.

Purified CXCL12-WT-SORT, CXCL12-LD-SORT and CCL2-SORT proteins were then sortagged with a five amino acid acyl acceptor peptide having the sequence GGGWpG where pG is propargyl glycine. Sortagging extends the C-terminus of the wild-type chemokine is by nine amino acids with the sequence LPETGGGWpG. Briefly, CXCL12-WT-SORT, CXCL12-LD-SORT or CCL2-SORT was solubilized in 50 mM Tris pH 7.4 containing 150 mM sodium chloride and 10 mM calcium chloride and mixed with a 2.5 molar excess of the acyl acceptor peptide. Calcium-dependent sortase A (86) was added at a molar ratio of 0.03:1 of sortase A:chemokine and the reaction incubated at 22° C for 15 minutes. The reaction was quenched by the addition of ethylenediaminetetraacetic acid to a final concentration of 30 mM and the sortagged product purified by reverse-phase HPLC

using a 21-42% acetonitrile gradient in 0.1% trifluoracetic acid. Purified products were lyophilized and their identity confirmed by LTQ-MS.

Copper-catalyzed azide-alkyne click chemistry (87) was used to couple the azide containing fluorescent dye AF647 (Click Chemistry Tools, Scottsdale, AZ) to the alkyne group present in propargyl glycine. Briefly, chemokines with the LPETGGGWpG extended C-terminus were solubilized in 50 mM HEPES pH 7.4 and mixed with a 1.2 molar excess of AF647. Reactions were run according to the protocol of Presolski *et al.* (87) for 15 minutes at room temperature and purified by reverse-phase HPLC using a 21-42% acetonitrile gradient in 0.1% trifluoracetic acid. Purified products were lyophilized and their identity confirmed by LTQ-MS.

ACKR1$^{N\text{-}term}$ production

DNA coding for the N-terminus of ACKR1, ACKR1$^{N\text{-}term}$, consisting of residues 1-60 with alanine substitutions at Cys^{4}, Cys^{51} and Cys^{54} was cloned into pQE30 with a N-terminal polyhistidine-SUMO fusion tag. The polyhistidine-SUMO tagged ACKR1$^{N\text{-}term}$ was expressed in E. coli BL21 pREP4 in 3 L of either luria broth or ^{15}N or ^{15}N/^{13}C M9 minimal media, with expression induced at an optical density at 600 nm of 0.75 using 1 mM isopropyl-beta-D-thiogalactopyranoside (IPTG) and growth occurring overnight at 25° °C. The cell pellet was resuspended in 30 mL of buffer A (50 mM sodium phosphate pH 7.2 containing 300 mM sodium chloride, 10 mM imidazole, 0.02% sodium azide, and protease inhibitor cocktail) and lysed with three passes through a French press or with sonication. The lysate was clarified using centrifugation (30 min at 15,000×g) and the supernatant bound to 8 mL of nickel agarose affinity resin. The resin was washed with 50 mL of buffer A and eluted with 14 mL of buffer B (50 mM sodium phosphate pH 7.2 containing 300 mM sodium chloride, 500 mM imidazole, and 0.02% sodium azide). The elution was dialyzed against 50 mM sodium phosphate pH 7.2 containing 100 mM sodium chloride, and 0.02% sodium azide overnight and then digested with ~400 μg of ULP1. The ACKR1$^{N\text{-}term}$ was separated from the polyhistidine-SUMO fusion protein by collecting the flow through after applying the digestion to 8 mL of nickel agarose affinity resin. The ACKR1$^{N\text{-}term}$ was further purified on a C18 column using reverse phase high performance liquid chromatography eluting with increasing concentrations of acetonitrile in aqueous 0.1% trifluoroacetic acid. The eluted ACKR1$^{N\text{-}term}$ was lyophilized and its identity confirmed by LTQ-MS. Purified protein was stored at −20° °C.

NMR

NMR spectroscopic data was collected at the NMR facility at the Medical College of Wisconsin on a Bruker Avance III 600 MHz spectrometer equipped with ^{1}H/^{13}C/^{15}N Cryoprobe® at 25 °C. Backbone chemical shift assignments for the ACKR1$^{N\text{-}term}$ (21) were confirmed using a 1 mM [U-^{15}N/^{13}C] ACKR1$^{N\text{-}term}$ in NMR buffer (20 mM deuterated MES pH 6.5 containing 10% D_2O, and 0.02 % NaN_3). Standard protein NMR methods were used for assigning ACKR1$^{N\text{-}term}$ amide and carbon backbone chemical shift assignments (53).

For NMR titrations, 50 μM [U-^{15}N] ACKR1$^{N\text{-}term}$ in NMR buffer was titrated with incremental additions of either CXCL12-LM, CXCL12-WT, or CXCL12-LD (0, 10, 25, 50, 75, 100 and 200 μM) and monitored using ^{15}N-^{1}H heteronuclear single quantum coherence (HSQC) spectra. Similarly, 50 μM [U-^{15}N] CXCL12-LM, CXCL12-WT, or CXCL12-LD was titrated with incremental additions of unlabeled ACKR1$^{N\text{-}term}$ (0, 25, 50, 75, 100, 200, and 400 μM) and monitored using ^{15}N-^{1}H HSQC spectra. Chemokine assignments were obtained from the following references (45, 51, 52, 88).

ITC

The isothermal titration calorimetry data was collected on a Microcal VP-ITC. Prior to running the experiments, all proteins and peptides were dialyzed in a Slide-A-lyser mini dialysis unit with a 2,000 MWCO against 20 mM MES at pH 6.5. Chemokine proteins, CXCL12-LM, CXCL12-WT or CXCL12-LD, were diluted to 20 μM and ACKR1$^{N\text{-}term}$ was diluted to 200 μM using dialysis buffer. The chemokine solution was placed in the cell and titrated by injecting 10 μL of ACKR1$^{N\text{-}term}$ with a 210 second spacing, a reference power of 10 μcal/sec, stirring of 307 rpm and a temperature set at 26°C. Origin software using the one-site or sequential binding model was used for data fitting.

MDCK cells

The full-length sequence of human ACKR1 was amplified by PCR using pCMV-ACKR1 (OriGene, Rockville, MD, USA) and the specific primers (forward: 5’ GACCCAAGCTTCATTACGATGGGGAACTGTCTGCACAGGG and reverse 5’: CCG CTC TCG AGT CCA CCGGATTTGCTTCCAAGGGTGTCCAG) and subcloned into the HindIII and XhoI sites of the pcDNA3 vector. MDCK cells were stably transfected with pcDNA3-ACKR1 using the Neon transfection system (Thermo Fisher Scientific). 24 hours later, transfected cells were sorted into single cell-suspension based on ACKR1 expression using an ACKR1 antibody (NaM185-2C3, BD Bioscience), expanded in selection medium (400 μg/ml G418) and re-sorted for ACKR1 expression after one week. Cells were further maintained in DMEM supplemented with 400 μg/ml G418. Untransfected MDCK cells were used as control and cultured in DMEM.

Human blood samples

Blood was collected in EDTA-coated tubes from healthy volunteers as approved by the ethical committee of QMUL London following written consent. To determine the expression of Duffy antigen on erythrocytes, whole blood was stained with mouse monoclonal anti-ACKR1 (clone NaM185-2C3, BD Biosciences), mouse monoclonal anti-CXCR4 (clone 12G5, Biolegend) and mouse monoclonal anti-CD235a (clone HI264, Biolegend).

Chemokine binding assay

For direct CXCL12-LD-AF647 binding, cells were incubated with 111, 333 or 1000 nM CXCL12-LD-AF647 for 45min at room temperature (RT). Cells were washed, resuspended in flow buffer (0.4 % PFA, 0.5 % BSA, 2mM EDTA in PBS) and analyzed on a FORTESSA (BD) flow cytometry. Mean fluorescence intensity (MFI) ratio was normalized to control baseline absent of CXCL12-LD-AF647 and depicted as percentage of maximum MFIR.

For competitive binding assays, cells were equilibrated with unlabeled 333 or 1000 nM CXCL12-WT or CXCL12-LD for 15min at 24 °C followed by 20nM CCL2-AF647 (Almac) for 45min at 24 °C. Cells were washed, stained for ACKR1 or erythrocyte markers and analyzed by flow cytometry. Specific binding of CCL2 was calculated as MFI of A647-conjugated chemokine in ACKR1 non-expressing and expressing groups, normalized for values without competitor and depicted as mean percent inhibition.

Live cell imaging

MDCK were grown overnight on glass bottom Cellview cell culture dishes® (Greiner Bio-One). Whole blood from healthy individuals was immobilized on poly-l-lysin coated Cellview cell culture dishes®. Cells were stained with HOECHST DNA dye and mouse monoclonal anti-ACKR1 (clone NaM185-2C3, BD Biosciences) where indicated. Cells were live-imaged in the presence of 100 nM CCL2-AF647 or 200nM CXCL12-LD-AF67 in a heat-controlled chamber at 37°C with 5% CO2 in 0.5% BSA-containing PBS using 40x oil immersion objective and a Zeiss 800 microscope (Zeiss, Jena, Germany). During long term time-lapse images were acquired every 5 min and a step size of 1 μm.

Statistical analysis

Statistics were performed using GraphPad Prism 8. Normal distribution was determined using the Kolmogorov–Smirnov test. Two normally distributed groups were compared using t-test. Nonparametric data sets were analyzed by Wilcoxon signed-rank tests for paired analysis or Mann-Whitney test for unpaired analysis. Grouped data was analyzed with two-way ANOVA with multiple comparison post-hoc tests. Results were considered significantly different when $P < 0.05$, with values at $P < 0.05$ marked as *, $P < 0.01$ as **, $P < 0.001$ as *** and $P < 0.0001$ as ****.

Supplementary Material

Refer to Web version on PubMed Central for supplementary material.

Acknowledgments:

We would like to acknowledge expert help with confocal microscopy studies by Rebecca Saleeb, CMR Advanced Bio-Imaging Facility, QMUL, and we thank Pontian E. Adogamhe and Gabriela J. Cordova of UW-Whitewater for technical assistance.

Funding:

The work on this project has been supported by the Wellcome Trust Investigator Award 200817/Z/16/Z to AR; Sinergia grant of the Swiss National Science Foundation CRSII3 160719 to DFL and AR; Versus Arthritis Endowment to AR; National Institutes of Health (USA) research grant R01 AI058072 to BFV, shared instrumentation grant S10 OD020000, and training grant T32 GM080202 to KSC.

Abbreviations Page

ACKR1	atypical chemokine receptor 1
ACKR1$^{N\text{-}term}$	ACKR1 N-terminal peptide residues 1-60
ACKR3	atypical chemokine receptor 3

CCL2	CC chemokine ligand 2
CXCL12	CXC chemokine ligand 12
CXCL12-LD	CXCL12 locked dimer
CXCL12-LM	CXCL12 locked monomer
CXCL12-WT	CXCL12 wild type
CXCR4	CXC chemokine receptor 4
DARC	Duffy antigen / receptor of chemokines
DBP	Duffy binding protein
GPCR	G-protein coupled receptor
HSQC	heteronuclear single quantum coherence spectra
ITC	isothermal titration calorimetry
NMR	nuclear magnetic resonance
RBC	red blood cells
SDF-1	Stromal cell derived factor 1
ULP1	Ubiquitin like protease

References

1. Rot A, von Andrian UH, Chemokines in innate and adaptive host defense: basic chemokinese grammar for immune cells. Annu Rev Immunol 22, 891–928 (2004). [PubMed: 15032599]
2. Ulvmar MH, Hub E, Rot A, Atypical chemokine receptors. Exp Cell Res 317, 556–568 (2011). [PubMed: 21272574]
3. Nagasawa T, Kikutani H, Kishimoto T, Molecular cloning and structure of a pre-B-cell growth-stimulating factor. Proc Natl Acad Sci U S A 91, 2305–2309 (1994). [PubMed: 8134392]
4. Tashiro K, Tada H, Heilker R, Shirozu M, Nakano T, Honjo T, Signal sequence trap: a cloning strategy for secreted proteins and type I membrane proteins. Science 261, 600–603 (1993). [PubMed: 8342023]
5. Gomariz A, Helbling PM, Isringhausen S, Suessbier U, Becker A, Boss A, Nagasawa T, Paul G, Goksel O, Szekely G, Stoma S, Norrelykke SF, Manz MG, Nombela-Arrieta C, Quantitative spatial analysis of haematopoiesis-regulating stromal cells in the bone marrow microenvironment by 3D microscopy. Nat Commun 9, 2532 (2018). [PubMed: 29955044]
6. Nagasawa T, Hirota S, Tachibana K, Takakura N, Nishikawa S, Kitamura Y, Yoshida N, Kikutani H, Kishimoto T, Defects of B-cell lymphopoiesis and bone-marrow myelopoiesis in mice lacking the CXC chemokine PBSF/SDF-1. Nature 382, 635–638 (1996). [PubMed: 8757135]
7. Ma Q, Jones D, Borghesani PR, Segal RA, Nagasawa T, Kishimoto T, Bronson RT, Springer TA, Impaired B-lymphopoiesis, myelopoiesis, and derailed cerebellar neuron migration in CXCR4- and SDF-1-deficient mice. Proc Natl Acad Sci U S A 95, 9448–9453 (1998). [PubMed: 9689100]
8. Tachibana K, Hirota S, Iizasa H, Yoshida H, Kawabata K, Kataoka Y, Kitamura Y, Matsushima K, Yoshida N, Nishikawa S, Kishimoto T, Nagasawa T, The chemokine receptor CXCR4 is essential for vascularization of the gastrointestinal tract. Nature 393, 591–594 (1998). [PubMed: 9634237]

9. Sierro F, Biben C, Martinez-Munoz L, Mellado M, Ransohoff RM, Li M, Woehl B, Leung H, Groom J, Batten M, Harvey RP, Martinez AC, Mackay CR, Mackay F, Disrupted cardiac development but normal hematopoiesis in mice deficient in the second CXCL12/SDF-1 receptor, CXCR7. Proc Natl Acad Sci U S A 104, 14759–14764 (2007). [PubMed: 17804806]
10. Gerrits H, van Ingen Schenau DS, Bakker NE, van Disseldorp AJ, Strik A, Hermens LS, Koenen TB, Krajnc-Franken MA, Gossen JA, Early postnatal lethality and cardiovascular defects in CXCR7-deficient mice. Genesis 46, 235–245 (2008). [PubMed: 18442043]
11. Janssens R, Struyf S, Proost P, The unique structural and functional features of CXCL12. Cell Mol Immunol 15, 299–311 (2018). [PubMed: 29082918]
12. Ray P, Lewin SA, Mihalko LA, Lesher-Perez SC, Takayama S, Luker KE, Luker GD, Secreted CXCL12 (SDF-1) forms dimers under physiological conditions. Biochem J 442, 433–442 (2012). [PubMed: 22142194]
13. Fermas S, Gonnet F, Sutton A, Charnaux N, Mulloy B, Du Y, Baleux F, Daniel R, Sulfated oligosaccharides (heparin and fucoidan) binding and dimerization of stromal cell-derived factor-1 (SDF-1/CXCL 12) are coupled as evidenced by affinity CE-MS analysis. Glycobiology 18, 1054–1064 (2008). [PubMed: 18796646]
14. Drury LJ, Ziarek JJ, Gravel S, Veldkamp CT, Takekoshi T, Hwang ST, Heveker N, Volkman BF, Dwinell MB, Monomeric and dimeric CXCL12 inhibit metastasis through distinct CXCR4 interactions and signaling pathways. Proc Natl Acad Sci U S A 108, 17655–17660 (2011). [PubMed: 21990345]
15. Cutbush M, Mollison PL, The Duffy blood group system. Heredity (Edinb) 4, 383–389 (1950). [PubMed: 14802995]
16. Haynes JD, Dalton JP, Klotz FW, McGinniss MH, Hadley TJ, Hudson DE, Miller LH, Receptor-like specificity of a Plasmodium knowlesi malarial protein that binds to Duffy antigen ligands on erythrocytes. J Exp Med 167, 1873–1881 (1988). [PubMed: 2838562]
17. Miller LH, Mason SJ, Clyde DF, McGinniss MH, The resistance factor to Plasmodium vivax in blacks. The Duffy-blood-group genotype, FyFy. N Engl J Med 295, 302–304 (1976). [PubMed: 778616]
18. Horuk R, Chitnis CE, Darbonne WC, Colby TJ, Rybicki A, Hadley TJ, Miller LH, A receptor for the malarial parasite Plasmodium vivax: the erythrocyte chemokine receptor. Science 261, 1182–1184 (1993). [PubMed: 7689250]
19. Miller LH, Mason SJ, Dvorak JA, McGinniss MH, Rothman IK, Erythrocyte receptors for (Plasmodium knowlesi) malaria: Duffy blood group determinants. Science 189, 561–563 (1975). [PubMed: 1145213]
20. Batchelor JD, Zahm JA, Tolia NH, Dimerization of Plasmodium vivax DBP is induced upon receptor binding and drives recognition of DARC. Nat Struct Mol Biol 18, 908–914 (2011). [PubMed: 21743458]
21. Batchelor JD, Malpede BM, Omattage NS, DeKoster GT, Henzler-Wildman KA, Tolia NH, Red blood cell invasion by Plasmodium vivax: structural basis for DBP engagement of DARC. PLoS Pathog 10, e1003869 (2014). [PubMed: 24415938]
22. Urusova D, Carias L, Huang Y, Nicolete VC, Popovici J, Roesch C, Salinas ND, Dechavanne S, Witkowski B, Ferreira MU, Adams JH, Gross ML, King CL, Tolia NH, Structural basis for neutralization of Plasmodium vivax by naturally acquired human antibodies that target DBP. Nat Microbiol 4, 1486–1496 (2019). [PubMed: 31133752]
23. Darbonne WC, Rice GC, Mohler MA, Apple T, Hebert CA, Valente AJ, Baker JB, Red blood cells are a sink for interleukin 8, a leukocyte chemotaxin. J Clin Invest 88, 1362–1369 (1991). [PubMed: 1918386]
24. Neote K, Mak JY, Kolakowski LF Jr., Schall TJ, Functional and biochemical analysis of the cloned Duffy antigen: identity with the red blood cell chemokine receptor. Blood 84, 44–52 (1994). [PubMed: 7517217]
25. Szabo MC, Soo KS, Zlotnik A, Schall TJ, Chemokine class differences in binding to the Duffy antigen-erythrocyte chemokine receptor. J Biol Chem 270, 25348–25351 (1995). [PubMed: 7592697]

26. Peiper SC, Wang ZX, Neote K, Martin AW, Showell HJ, Conklyn MJ, Ogborne K, Hadley TJ, Lu ZH, Hesselgesser J, Horuk R, The Duffy antigen/receptor for chemokines (DARC) is expressed in endothelial cells of Duffy negative individuals who lack the erythrocyte receptor. J Exp Med 181, 1311–1317 (1995). [PubMed: 7699323]
27. Bachelerie F, Graham GJ, Locati M, Mantovani A, Murphy PM, Nibbs R, Rot A, Sozzani S, Thelen M, New nomenclature for atypical chemokine receptors. Nat Immunol 15, 207–208 (2014). [PubMed: 24549061]
28. Tournamille C, Colin Y, Cartron JP, Le Van Kim C, Disruption of a GATA motif in the Duffy gene promoter abolishes erythroid gene expression in Duffy-negative individuals. Nat Genet 10, 224–228 (1995). [PubMed: 7663520]
29. Duchene J, Novitzky-Basso I, Thiriot A, Casanova-Acebes M, Bianchini M, Etheridge SL, Hub E, Nitz K, Artinger K, Eller K, Caamano J, Rulicke T, Moss P, Megens RTA, von Andrian UH, Hidalgo A, Weber C, Rot A, Atypical chemokine receptor 1 on nucleated erythroid cells regulates hematopoiesis. Nat Immunol 18, 753–761 (2017). [PubMed: 28553950]
30. Hadley TJ, Lu ZH, Wasniowska K, Martin AW, Peiper SC, Hesselgesser J, Horuk R, Postcapillary venule endothelial cells in kidney express a multispecific chemokine receptor that is structurally and functionally identical to the erythroid isoform, which is the Duffy blood group antigen. J Clin Invest 94, 985–991 (1994). [PubMed: 8083383]
31. Chaudhuri A, Nielsen S, Elkjaer ML, Zbrzezna V, Fang F, Pogo AO, Detection of Duffy antigen in the plasma membranes and caveolae of vascular endothelial and epithelial cells of nonerythroid organs. Blood 89, 701–712 (1997). [PubMed: 9002974]
32. Thiriot A, Perdomo C, Cheng G, Novitzky-Basso I, McArdle S, Kishimoto JK, Barreiro O, Mazo I, Triboulet R, Ley K, Rot A, von Andrian UH, Differential DARC/ACKR1 expression distinguishes venular from non-venular endothelial cells in murine tissues. BMC Biol 15, 45 (2017). [PubMed: 28526034]
33. Pruenster M, Mudde L, Bombosi P, Dimitrova S, Zsak M, Middleton J, Richmond A, Graham GJ, Segerer S, Nibbs RJ, Rot A, The Duffy antigen receptor for chemokines transports chemokines and supports their promigratory activity. Nat Immunol 10, 101–108 (2009). [PubMed: 19060902]
34. Horuk R, Martin AW, Wang Z, Schweitzer L, Gerassimides A, Guo H, Lu Z, Hesselgesser J, Perez HD, Kim J, Parker J, Hadley TJ, Peiper SC, Expression of chemokine receptors by subsets of neurons in the central nervous system. J Immunol 158, 2882–2890 (1997). [PubMed: 9058825]
35. Jilma-Stohlawetz P, Homoncik M, Drucker C, Marsik C, Rot A, Mayr WR, Seibold B, Jilma B, Fy phenotype and gender determine plasma levels of monocyte chemotactic protein. Transfusion 41, 378–381 (2001). [PubMed: 11274594]
36. Colditz IG, Schneider MA, Pruenster M, Rot A, Chemokines at large: in-vivo mechanisms of their transport, presentation and clearance. Thromb Haemost 97, 688–693 (2007). [PubMed: 17479178]
37. Fukuma N, Akimitsu N, Hamamoto H, Kusuhara H, Sugiyama Y, Sekimizu K, A role of the Duffy antigen for the maintenance of plasma chemokine concentrations. Biochem Biophys Res Commun 303, 137–139 (2003). [PubMed: 12646177]
38. Mayr FB, Spiel AO, Leitner JM, Firbas C, Kliegel T, Jilma-Stohlawetz P, Derendorf H, Jilma B, Duffy antigen modifies the chemokine response in human endotoxemia. Crit Care Med 36, 159–165 (2008). [PubMed: 18007272]
39. Mei J, Liu Y, Dai N, Favara M, Greene T, Jeyaseelan S, Poncz M, Lee JS, Worthen GS, CXCL5 regulates chemokine scavenging and pulmonary host defense to bacterial infection. Immunity 33, 106–117 (2010). [PubMed: 20643340]
40. Rot A, Contribution of Duffy antigen to chemokine function. Cytokine Growth Factor Rev 16, 687–694 (2005). [PubMed: 16054417]
41. Novitzky-Basso I, Rot A, Duffy antigen receptor for chemokines and its involvement in patterning and control of inflammatory chemokines. Front Immunol 3, 266 (2012). [PubMed: 22912641]
42. Crump MP, Gong JH, Loetscher P, Rajarathnam K, Amara A, Arenzana-Seisdedos F, Virelizier JL, Baggiolini M, Sykes BD, Clark-Lewis I, Solution structure and basis for functional activity of stromal cell-derived factor-1; dissociation of CXCR4 activation from binding and inhibition of HIV-1. Embo J 16, 6996–7007. (1997). [PubMed: 9384579]

43. Kleist AB, Getschman AE, Ziarek JJ, Nevins AM, Gauthier PA, Chevigne A, Szpakowska M, Volkman BF, New paradigms in chemokine receptor signal transduction: Moving beyond the two-site model. Biochem Pharmacol 114, 53–68 (2016). [PubMed: 27106080]
44. Gustavsson M, Dyer DP, Zhao C, Handel TM, Kinetics of CXCL12 binding to atypical chemokine receptor 3 reveal a role for the receptor N terminus in chemokine binding. Sci Signal 12, (2019).
45. Veldkamp CT, Seibert C, Peterson FC, De la Cruz NB, Haugner JC 3rd, Basnet H, Sakmar TP, Volkman BF, Structural basis of CXCR4 sulfotyrosine recognition by the chemokine SDF-1/CXCL12. Sci Signal 1, (2008).
46. Veldkamp CT, Seibert C, Peterson FC, Sakmar TP, Volkman BF, Recognition of a CXCR4 sulfotyrosine by the chemokine stromal cell-derived factor-1alpha (SDF-1alpha/CXCL12). J Mol Biol 359, 1400–1409 (2006). [PubMed: 16725153]
47. Millard CJ, Ludeman JP, Canals M, Bridgford JL, Hinds MG, Clayton DJ, Christopoulos A, Payne RJ, Stone MJ, Structural basis of receptor sulfotyrosine recognition by a CC chemokine: the N-terminal region of CCR3 bound to CCL11/eotaxin-1. Structure 22, 1571–1581 (2014). [PubMed: 25450766]
48. Tan JH, Ludeman JP, Wedderburn J, Canals M, Hall P, Butler SJ, Taleski D, Christopoulos A, Hickey MJ, Payne RJ, Stone MJ, Tyrosine sulfation of chemokine receptor CCR2 enhances interactions with both monomeric and dimeric forms of the chemokine monocyte chemoattractant protein-1 (MCP-1). J Biol Chem 288, 10024–10034 (2013). [PubMed: 23408426]
49. Ludeman JP, Stone MJ, The structural role of receptor tyrosine sulfation in chemokine recognition. Br J Pharmacol 171, 1167–1179 (2014). [PubMed: 24116930]
50. Abayev M, Rodrigues J, Srivastava G, Arshava B, Jaremko L, Jaremko M, Naider F, Levitt M, Anglister J, The solution structure of monomeric CCL5 in complex with a doubly sulfated N-terminal segment of CCR5. FEBS J 285, 1988–2003 (2018). [PubMed: 29619777]
51. Ziarek JJ, Kleist AB, London N, Raveh B, Montpas N, Bonneterre J, St-Onge G, DiCosmo-Ponticello CJ, Koplinski CA, Roy I, Stephens B, Thelen S, Veldkamp CT, Coffman FD, Cohen MC, Dwinell MB, Thelen M, Peterson FC, Heveker N, Volkman BF, Structural basis for chemokine recognition by a G protein-coupled receptor and implications for receptor activation. Sci Signal 10, (2017).
52. Ziarek JJ, Getschman AE, Butler SJ, Taleski D, Stephens B, Kufareva I, Handel TM, Payne RJ, Volkman BF, Sulfopeptide probes of the CXCR4/CXCL12 interface reveal oligomer-specific contacts and chemokine allostery. ACS Chem Biol 8, 1955–1963 (2013). [PubMed: 23802178]
53. Markley JL, Ulrich EL, Westler WM, Volkman BF, Macromolecular structure determination by NMR spectroscopy. Methods Biochem Anal 44, 89–113 (2003). [PubMed: 12647383]
54. Gardner L, Patterson AM, Ashton BA, Stone MA, Middleton J, The human Duffy antigen binds selected inflammatory but not homeostatic chemokines. Biochem Biophys Res Commun 321, 306–312 (2004). [PubMed: 15358176]
55. Klei TRL, Aglialoro F, Mul FPJ, Tol S, Ligthart PC, Seignette IM, Geissler J, van den Akker E, van Bruggen R, Differential interaction between DARC and SDF-1 on erythrocytes and their precursors. Sci Rep 9, 16245 (2019). [PubMed: 31700087]
56. Palmer AG 3rd, Chemical exchange in biomacromolecules: past, present, and future. J Magn Reson 241, 3–17 (2014). [PubMed: 24656076]
57. Veldkamp CT, Peterson FC, Pelzek AJ, Volkman BF, The monomer-dimer equilibrium of stromal cell-derived factor-1 (CXCL 12) is altered by pH, phosphate, sulfate, and heparin. Protein Sci 14, 1071–1081 (2005). [PubMed: 15741341]
58. Rot A, In situ binding assay for studying chemokine interactions with endothelial cells. J Immunol Methods 273, 63–71 (2003). [PubMed: 12535798]
59. Apostolakis S, Chalikias GK, Tziakas DN, Konstantinides S, Erythrocyte Duffy antigen receptor for chemokines (DARC): diagnostic and therapeutic implications in atherosclerotic cardiovascular disease. Acta Pharmacol Sin 32, 417–424 (2011). [PubMed: 21441947]
60. Ameti R, Melgrati S, Radice E, Cameroni E, Hub E, Thelen S, Rot A, Thelen M, Characterization of a chimeric chemokine as a specific ligand for ACKR3. J Leukoc Biol 104, 391–400 (2018). [PubMed: 29601107]

61. Webb LM, Ehrengruber MU, Clark-Lewis I, Baggiolini M, Rot A, Binding to heparan sulfate or heparin enhances neutrophil responses to interleukin 8. Proc Natl Acad Sci U S A 90, 7158–7162 (1993). [PubMed: 8346230]

62. Rot A, Chemokine patterning by glycosaminoglycans and interceptors. Front Biosci (Landmark Ed) 15, 645–660 (2010). [PubMed: 20036838]

63. Vogt AM, Winter G, Wahlgren M, Spillmann D, Heparan sulphate identified on human erythrocytes: a Plasmodium falciparum receptor. Biochem J 381, 593–597 (2004). [PubMed: 15209561]

64. Ziarek JJ, Veldkamp CT, Zhang F, Murray NJ, Kartz GA, Liang X, Su J, Baker JE, Linhardt RJ, Volkman BF, Heparin oligosaccharides inhibit chemokine (CXC motif) ligand 12 (CXCL12) cardioprotection by binding orthogonal to the dimerization interface, promoting oligomerization, and competing with the chemokine (CXC motif) receptor 4 (CXCR4) N terminus. J Biol Chem 288, 737–746 (2013). [PubMed: 23148226]

65. Gustavsson M, Wang L, van Gils N, Stephens BS, Zhang P, Schall TJ, Yang S, Abagyan R, Chance MR, Kufareva I, Handel TM, Structural basis of ligand interaction with atypical chemokine receptor 3. Nat Commun 8, 14135 (2017). [PubMed: 28098154]

66. Proudfoot AEI, Johnson Z, Bonvin P, Handel TM, Glycosaminoglycan Interactions with Chemokines Add Complexity to a Complex System. Pharmaceuticals (Basel) 10, (2017).

67. Salanga CL, Handel TM, Chemokine oligomerization and interactions with receptors and glycosaminoglycans: the role of structural dynamics in function. Exp Cell Res 317, 590–601 (2011). [PubMed: 21223963]

68. Liang WG, Triandafillou CG, Huang TY, Zulueta MM, Banerjee S, Dinner AR, Hung SC, Tang WJ, Structural basis for oligomerization and glycosaminoglycan binding of CCL5 and CCL3. Proc Natl Acad Sci U S A 113, 5000–5005 (2016). [PubMed: 27091995]

69. Qin L, Kufareva I, Holden LG, Wang C, Zheng Y, Zhao C, Fenalti G, Wu H, Han GW, Cherezov V, Abagyan R, Stevens RC, Handel TM, Structural biology. Crystal structure of the chemokine receptor CXCR4 in complex with a viral chemokine. Science 347, 1117–1122 (2015). [PubMed: 25612609]

70. Wu B, Chien EY, Mol CD, Fenalti G, Liu W, Katritch V, Abagyan R, Brooun A, Wells P, Bi FC, Hamel DJ, Kuhn P, Handel TM, Cherezov V, Stevens RC, Structures of the CXCR4 chemokine GPCR with small-molecule and cyclic peptide antagonists. Science 330, 1066–1071 (2010). [PubMed: 20929726]

71. Tournamille C, Le Van Kim C, Gane P, Blanchard D, Proudfoot AE, Cartron JP, Colin Y, Close association of the first and fourth extracellular domains of the Duffy antigen/receptor for chemokines by a disulfide bond is required for ligand binding. J Biol Chem 272, 16274–16280 (1997). [PubMed: 9195930]

72. Kashiwazaki M, Tanaka T, Kanda H, Ebisuno Y, Izawa D, Fukuma N, Akimitsu N, Sekimizu K, Monden M, Miyasaka M, A high endothelial venule-expressing promiscuous chemokine receptor DARC can bind inflammatory, but not lymphoid, chemokines and is dispensable for lymphocyte homing under physiological conditions. Int Immunol 15, 1219–1227 (2003). [PubMed: 13679391]

73. Czerwinski M, Kern J, Grodecka M, Paprocka M, Krop-Watorek A, Wasniowska K, Mutational analysis of the N-glycosylation sites of Duffy antigen/receptor for chemokines. Biochem Biophys Res Commun 356, 816–821 (2007). [PubMed: 17382291]

74. Wang J, Babcock GJ, Choe H, Farzan M, Sodroski J, Gabuzda D, N-linked glycosylation in the CXCR4 N-terminus inhibits binding to HIV-1 envelope glycoproteins. Virology 324, 140–150 (2004). [PubMed: 15183061]

75. Chabot DJ, Chen H, Dimitrov DS, Broder CC, N-linked glycosylation of CXCR4 masks coreceptor function for CCR5-dependent human immunodeficiency virus type 1 isolates. J Virol 74, 4404–4413 (2000). [PubMed: 10756055]

76. Farzan M, Babcock GJ, Vasilieva N, Wright PL, Kiprilov E, Mirzabekov T, Choe H, The role of post-translational modifications of the CXCR4 amino terminus in stromal-derived factor 1 alpha association and HIV-1 entry. J Biol Chem 277, 29484–29489 (2002). [PubMed: 12034737]

77. Zheng Y, Han GW, Abagyan R, Wu B, Stevens RC, Cherezov V, Kufareva I, Handel TM, Structure of CC Chemokine Receptor 5 with a Potent Chemokine Antagonist Reveals Mechanisms of

Chemokine Recognition and Molecular Mimicry by HIV. Immunity 46, 1005–1017 e1005 (2017). [PubMed: 28636951]

78. Liu K, Wu L, Yuan S, Wu M, Xu Y, Sun Q, Li S, Zhao S, Hua T, Liu ZJ, Structural basis of CXC chemokine receptor 2 activation and signalling. Nature 585, 135–140 (2020). [PubMed: 32610344]
79. Sampath S, Carrico C, Janes J, Gurumoorthy S, Gibson C, Melcher M, Chitnis CE, Wang R, Schief WR, Smith JD, Glycan masking of Plasmodium vivax Duffy Binding Protein for probing protein binding function and vaccine development. PLoS Pathog 9, e1003420 (2013). [PubMed: 23853575]
80. Chakera A, Seeber RM, John AE, Eidne KA, Greaves DR, The duffy antigen/receptor for chemokines exists in an oligomeric form in living cells and functionally antagonizes CCR5 signaling through hetero-oligomerization. Mol Pharmacol 73, 1362–1370 (2008). [PubMed: 18230715]
81. Agarwal P, Isringhausen S, Li H, Paterson AJ, He J, Gomariz A, Nagasawa T, Nombela-Arrieta C, Bhatia R, Mesenchymal Niche-Specific Expression of Cxcl12 Controls Quiescence of Treatment-Resistant Leukemia Stem Cells. Cell Stem Cell 24, 769–784 e766 (2019). [PubMed: 30905620]
82. Schneider EH, Fowler SC, Lionakis MS, Swamydas M, Holmes G, Diaz V, Munasinghe J, Peiper SC, Gao JL, Murphy PM, Regulation of motor function and behavior by atypical chemokine receptor 1. Behav Genet 44, 498–515 (2014). [PubMed: 24997773]
83. Girbl T, Lenn T, Perez L, Rolas L, Barkaway A, Thiriot A, Del Fresno C, Lynam E, Hub E, Thelen M, Graham G, Alon R, Sancho D, von Andrian UH, Voisin MB, Rot A, Nourshargh S, Distinct Compartmentalization of the Chemokines CXCL1 and CXCL2 and the Atypical Receptor ACKR1 Determine Discrete Stages of Neutrophil Diapedesis. Immunity 49, 1062–1076 e1066 (2018). [PubMed: 30446388]
84. Veldkamp CT, Koplinski CA, Jensen DR, Peterson FC, Smits KM, Smith BL, Johnson SK, Lettieri C, Buchholz WG, Solheim JC, Volkman BF, Production of Recombinant Chemokines and Validation of Refolding. Methods Enzymol 570, 539–565 (2016). [PubMed: 26921961]
85. Antos JM, Truttmann MC, Ploegh HL, Recent advances in sortase-catalyzed ligation methodology. Curr Opin Struct Biol 38, 111–118 (2016). [PubMed: 27318815]
86. Chen I, Dorr BM, Liu DR, A general strategy for the evolution of bond-forming enzymes using yeast display. Proc Natl Acad Sci U S A 108, 11399–11404 (2011). [PubMed: 21697512]
87. Presolski SI, Hong VP, Finn MG, Copper-Catalyzed Azide-Alkyne Click Chemistry for Bioconjugation. Curr Protoc Chem Biol 3, 153–162 (2011). [PubMed: 22844652]
88. Veldkamp CT, Ziarek JJ, Su J, Basnet H, Lennertz R, Weiner JJ, Peterson FC, Baker JE, Volkman BF, Monomeric structure of the cardioprotective chemokine SDF-1/CXCL12. Protein Sci 18, 1359–1369 (2009). [PubMed: 19551879]

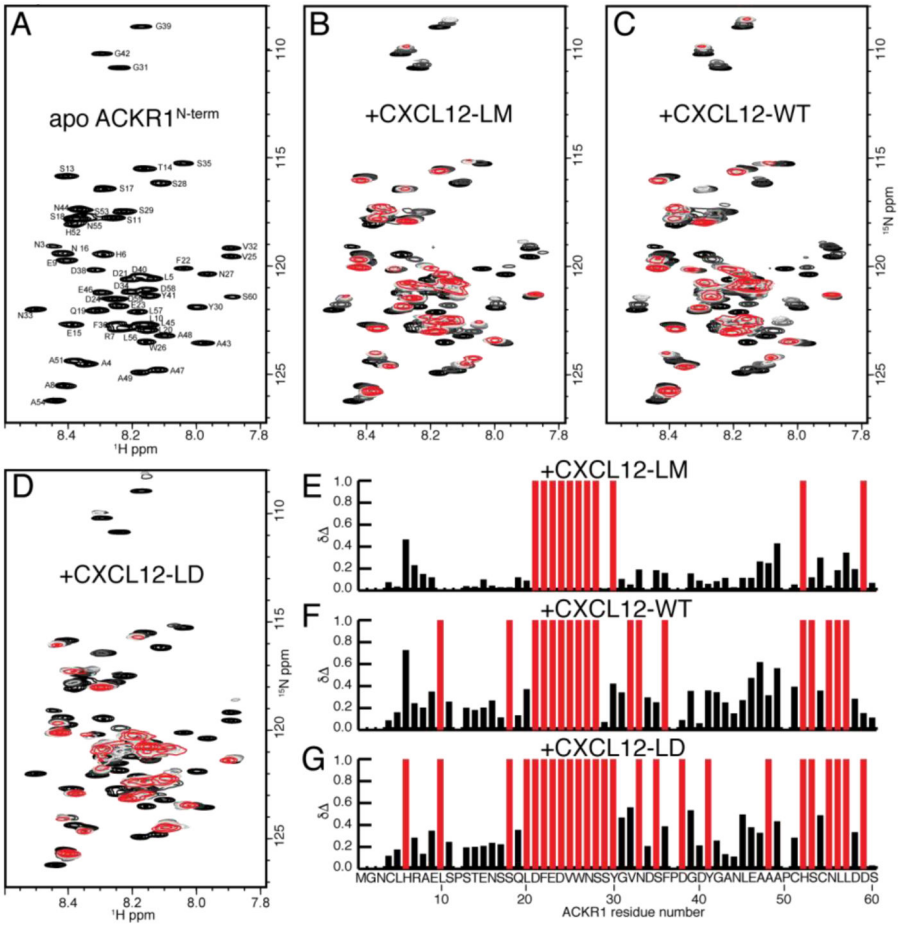

Figure 1. ACKR1$^{N\text{-}term}$ binds to CXCL12-LM, CXCL12-WT and CXCL12-LD.

(A) ^{15}N-^{1}H HSQC spectrum of 50 μM ^{15}N ACKR1N^{-term} alone. Overlays of ^{15}N-^{1}H HSQC spectra of 50 μM ^{15}N ACKR1$^{N\text{-}term}$ alone (black) or with increasing concentrations of CXCL12-LM **(B)**, CXCL12-WT **(C)**, or CXCL12-LD **(D)** (10, 25, 50, 75, and 100 μM in lightening grays and 200 μM in red). The resulting ACKR1$^{N\text{-}term}$ chemical shift perturbations induced by 200 μM CXCL12-LM **(E)**, CXCL12-WT **(F)**, and CXCL12-LD **(G)** are plotted versus ACKR1$^{N\text{-}term}$ residue number. Prolines and unobserved residues have a value of zero while amino acids whose amide cross peak broadened beyond detection during the titration have a value of 1 and are colored red.

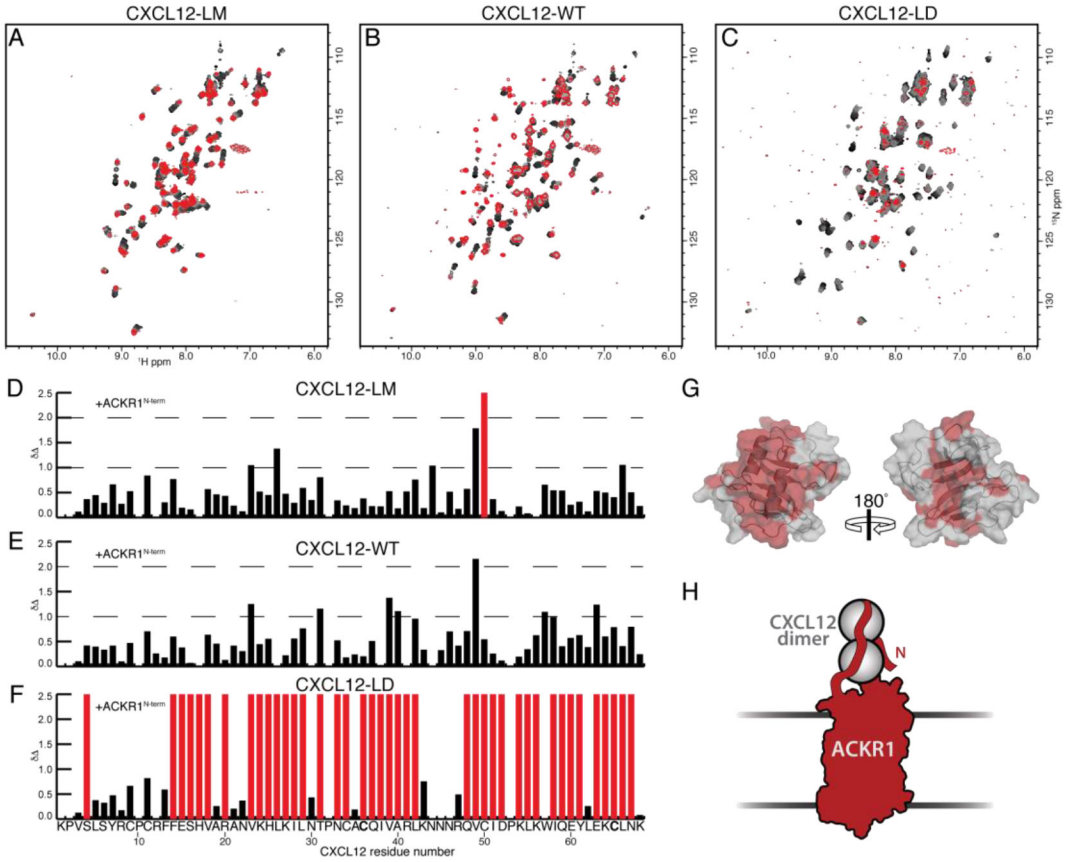

Figure 2. ACKR1$^{N\text{-}term}$ induced chemical shift perturbations in isotopically labeled locked monomer, wild type, or locked dimer CXCL12.

Overlays of 15N-1H HSQC spectra of 50 μM [U-15N] CXCL12-LM **(A)**, CXCL12-WT **(B)**, or CXCL12-LD **(C)** without (black) and with increasing concentrations of ACKR1$^{N\text{-}term}$ (10, 25, 50, 75, 100, and 200 μM lightening grays and 400 μM red). The resulting CXCL12-LM **(D)**, CXCL12-WT **(E)** and CXCL12-LD **(F)** chemical shift perturbations induced by 400 μM ACKR1$^{N\text{-}term}$ are plotted versus chemokine residue number with bar graph values of 2.5 and the color red indicating the residue broaden beyond detection during the titration. Residues with zero chemical shift change are either prolines or are not readily observed. **(G)** Chemical shifts are mapped in red onto the CXCL12 dimeric structure (PDB: 2K01) with schematic **(H)** of potential binding region.

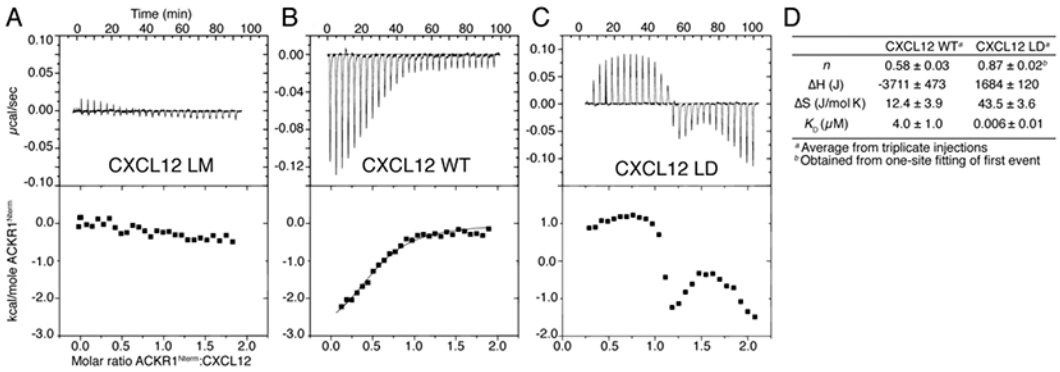

Figure 3. ACKR1$^{N\text{-}term}$ preferentially binds CXCL12 dimer.

Representative titrations with CXCL12 and ACKR1$^{N\text{-}term}$ displayed. **(A)** Injection of 200μM ACKR1$^{N\text{-}term}$ into 20μM CXCL12-LM. **(B)** Injection of 200μM ACKR1$^{N\text{-}term}$ into 20μM CXCL12-WT. **(C)** Injection of 200μM ACKR1$^{N\text{-}term}$ into 20μM CXCL12-LD. D) Average measurements from ITC determinations (N = 3) obtained through fitting using a one-site binding model for CXCL12-WT and a sequential binding model applied to the initial transition of CXCL12-LD in Origin are shown **(D)** ± the mean absolute error, except the calculated ΔS, which are shown ± the standard deviation.

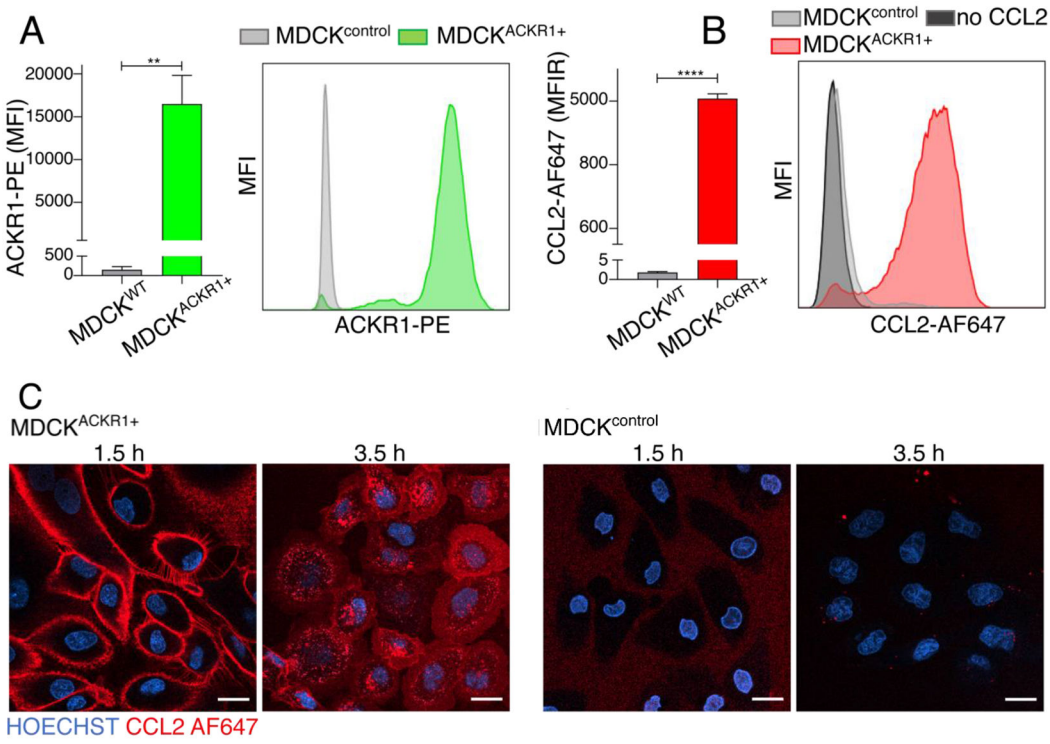

Figure 4. Expression of ACKR1 and its binding of CCL2 in transduced MDCK cells.

(A) The efficiency of ACKR1 expression in transfected MDCK ($MDCK^{ACKR1+}$) cells compared to parental control ($MDCK^{control}$) cells determined in flow cytometry by specific anti-human ACKR1 antibody. Mean fluorescence intensities (MFI) ± SD and representative histograms are shown (N = 3). **(B)** Chemokine binding of ACKR1 was assessed in flow cytometry by measuring the association of fluorescently labeled canonical ligand CCL2 (20 nM CCL2-AF647) with $MDCK^{ACKR1+}$ and $MDCK^{control}$ cells. Data shown as MFI ratios (MFIR) normalized to untreated controls ± SD and as representative histograms (N = 3). **(C)** Comparison of CCL2-AF647 binding to $MDCK^{ACKR1+}$ and $MDCK^{control}$ cells under confocal microscope. Representative images show the time course of cell binding and internalization following incubation with 20 nM CCL2-AF647 (N = 3) (scale bar 20 μm). T-tests were used. Significance values at $p < 0.05$ marked as *, $p < 0.01$ as **, $p < 0.001$ as *** and $p < 0.0001$ as ****.

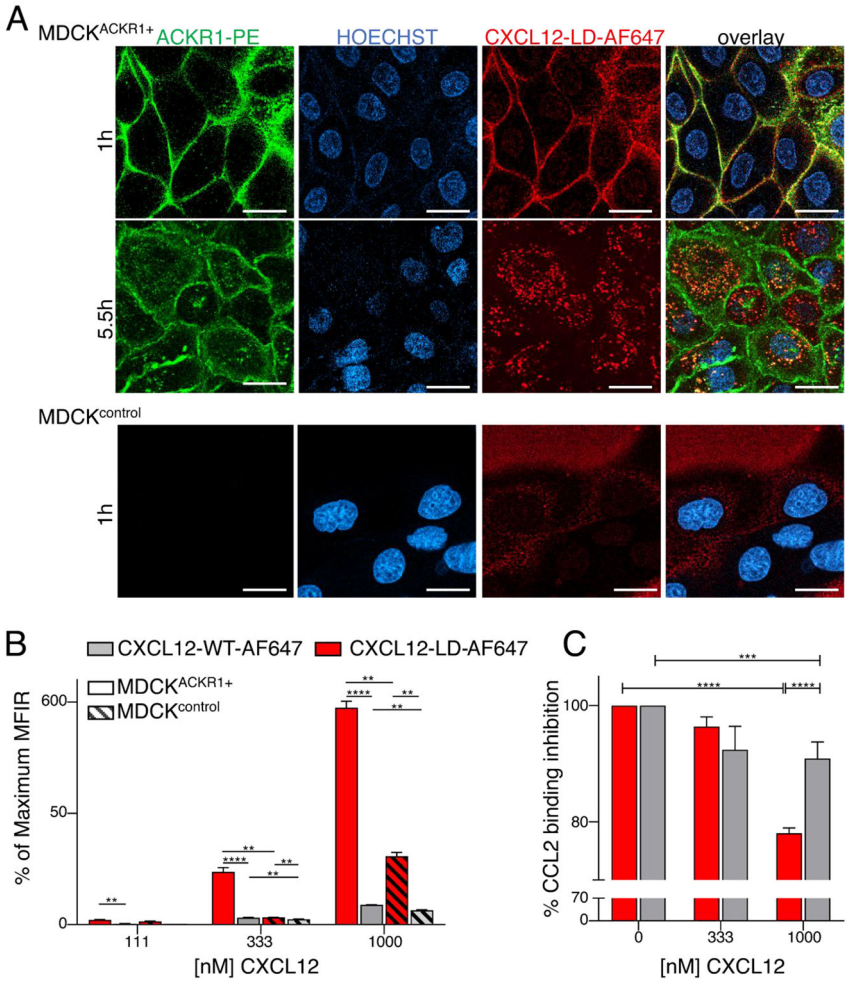

Figure 5. CXCL12-LD binds to ACKR1 on transfected MDCK cells.

(A) Time course comparison of ACKR1-dependent binding and internalization of CXCL12-LD-AF647 in MDCK^{ACKR1+} and MDCK^{control} cells observed in confocal microscopy. Representative images are shown (N = 3); scale bar 20 μm. **(B)** Dose-dependent binding of CXCL12-LD-AF647 and CXCL12-WT-AF647 to MDCK^{ACKR1+} and MDCK^{control} cells as measured in flow cytometry. Percentage of maximal mean fluorescence intensity ratios (MFIR ± SD) normalized to untreated control are shown (N = 3). **(C)** Comparison of inhibition by CXCL12-LD and CXCL12-WT of CCL2-AF647 (20 nM) binding to MDCK^{ACKR1+} measured in flow cytometry. Data shown as percent inhibition of mean fluorescence intensity normalized to individual untreated controls (mean ± SD; N = 3). Two-way ANOVA with Tukey's and Sidak's post-hoc tests were used. Significance: values at $p < 0.05$ marked as *, $p < 0.01$ as **, $p < 0.001$ as *** and $p < 0.0001$ as ****.

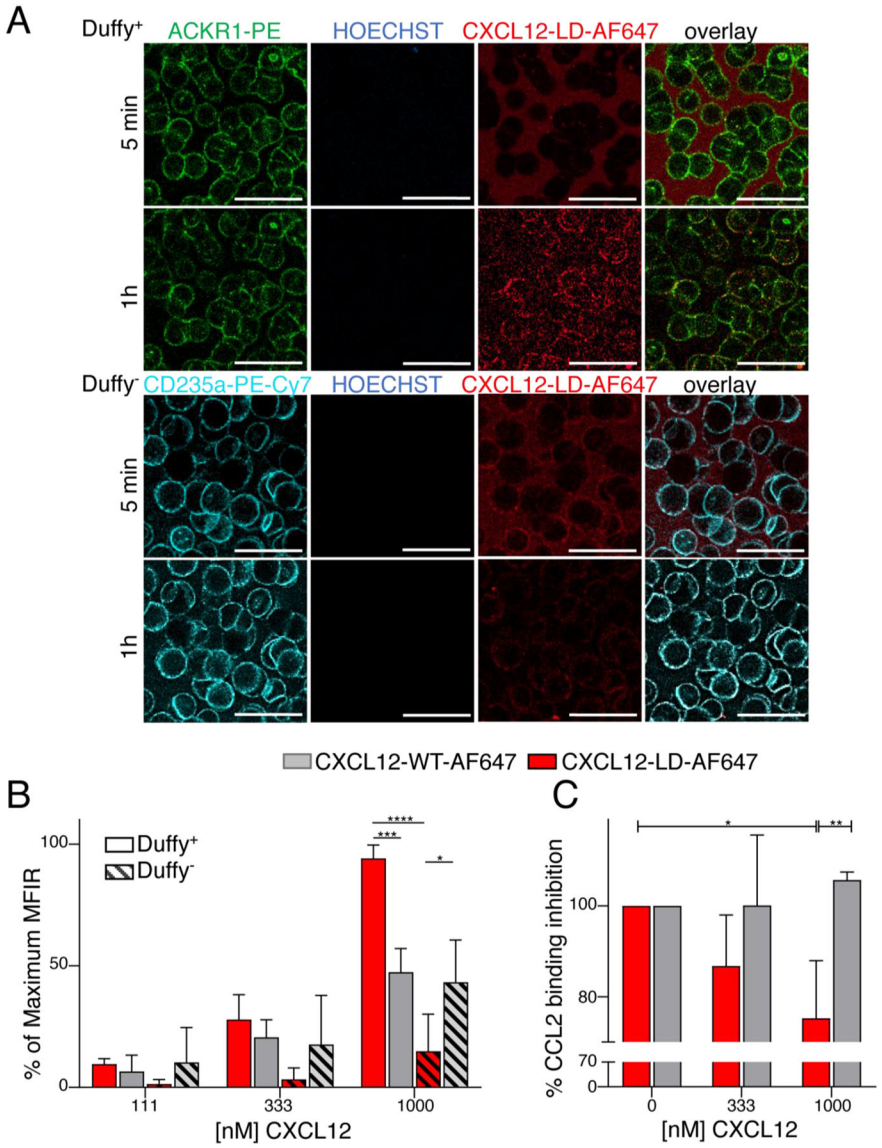

Figure 6. ACKR1-dependent binding of CXCL12-LD to primary human erythrocytes.

(A) Time course of CXCL12-LD-AF647 interactions with primary Duffy-positive and Duffy-negative human erythrocytes as observed in confocal microscopy. Representative images are shown (N = 3); scale bar 20 μm. **(B)** Dose-dependent binding of CXCL12-LD-AF647 and CXCL12-WT-AF647 to primary Duffy-positive human erythrocytes measured by flow cytometry. Data expressed as percentage of mean fluorescence intensity ratio (MFIR) normalized to the untreated control (± SD) (N = 3). **(C)** Flow cytometry comparison of dose -dependent inhibition of CCL2-AF647 (20 nM) binding to Duffy positive erythrocytes by CXCL12-LD and CXCL12-WT. Data shown as percent inhibition of mean fluorescence intensity normalized to individual untreated controls (mean ± SD; N = 3). Two-way ANOVA with Tukey's and Sidak's post-hoc tests were used. Significance; values at $p < 0.05$ marked as *, $p < 0.01$ as **, $p < 0.001$ as *** and $p < 0.0001$ as ****.